

1 **Elimination from Wastewater of Antibiotics Reserved for Hospital**
2 **Settings, with a Fenton Process Based on Zero-Valent Iron**

3
4 **Francesco Furia,^a Marco Minella,^a Fabio Gosetti,^b Francesco Turci,^a Raffaella**
5 **Sabatino,^c Andrea Di Cesare,^c Gianluca Corno,^c Davide Vione^{a*}**

6
7 *^a Dipartimento di Chimica, Università di Torino, Via Pietro Giuria 5,9, 10125 Torino, Italy.*

8 *^b Dipartimento di Scienze dell'Ambiente e della Terra, Università di Milano – Bicocca, Piazza della*
9 *Scienza 1, 20126 Milano, Italy.*

10 *^c Molecular Ecology Group, National Research Council of Italy, Water Research Institute, Largo*
11 *Tonolli 50, 28922, Verbania (VCO), Italy.*

12 * Corresponding author. E-mail: *davide.vione@unito.it*

13
14 ***Abstract***

15 The Fenton process activated by Zero Valent Iron (ZVI-Fenton) is shown here to effectively remove
16 antibiotics reserved for hospital settings (specifically used to treat antibiotic-resistant infections)
17 from wastewater, thereby helping in the fight against bacterial resistance. Effective degradation of
18 cefazolin, imipenem and vancomycin in real urban wastewater was achieved at pH 5, which is quite
19 near neutrality when compared with classic Fenton that works effectively at pH 3-4. The possibility
20 to operate successfully at pH 5 has several advantages compared to operation at lower pH values: (i)
21 lower reagent costs for pH adjustment; (ii) insignificant impact on wastewater conductivity, because
22 lesser acid is required to acidify and lesser or no base for neutralization; (iii) production of
23 undetectable dissolved Fe, which could otherwise be an issue for wastewater quality. The cost of
24 reagents for the treatment ranges between 0.04 and 0.07 \$ m⁻³, which looks very suitable for
25 practical applications. The structures of the degradation intermediates of the studied antibiotics and

26 their likely abundance suggest that, once the primary compound is eliminated, most of the potential
27 to trigger antibiotic action has been removed. Application of the ZVI-Fenton technique to
28 wastewater treatment could considerably lower the possibility for antibiotics to trigger the
29 development of resistance in bacteria.

30

31 **Keywords:** cefazolin; vancomycin; imipenem; wastewater remediation; advanced oxidation
32 processes; degradation products.

33

34 **1. INTRODUCTION**

35

36 The spread of antibiotic resistance (ABR) among bacteria is a growing threat that stems from a
37 combination of excessive prescriptions of antibiotics, incorrect disposal, use outside of the field of
38 human medicine, and slowing-down of research into the development of new drugs (Levy, 1998).
39 ABR could jeopardize the efficacy of antibiotics in future years, with the potential to produce many
40 casualties because of diseases or medical procedures that are presently regarded as trivial (Wiles,
41 2016; Cox and Worthington, 2017). The spread of ABR takes place at various levels and involves
42 many sectors of society (Cully, 2014; Cars, 2014; McCullough et al., 2016), including wastewater
43 treatment (Amador et al., 2015).

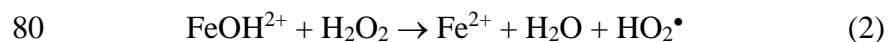
44 Wastewater is a major contributor to the spreading of ABR because it contains: (i) antibiotic
45 residues that are incompletely eliminated and end up in surface waters, where their concentration is
46 too low to kill bacteria but can still be high enough (up to several hundred $\mu\text{g L}^{-1}$ in the water
47 matrix; Zhao et al., 2017) to favor the onset of resistance (Bengtsson-Palme and Larsson, 2016),
48 and (ii) antibiotic-resistant bacteria and resistance genes (Rizzo et al., 2013). Unfortunately, the
49 present techniques used in wastewater treatment plants (WWTPs) are poorly effective at removing
50 biorecalcitrant compounds that include many contaminants of emerging concern (CECs), such as

51 the antibiotics, which are poorly compatible with biological treatment (Behera et al., 2011; Ahmed
52 et al., 2017; Richardson and Ternes, 2018). Moreover, the final step of wastewater disinfection is
53 often unable to totally eliminate resistant bacteria, and it could even select for antibiotic resistance
54 genes (Di Cesare et al., 2016).

55 A very important role in the fight against bacteria is played by the antibiotics reserved for hospital
56 settings. These antibiotics are used in hospitals to treat infections that are resistant to the other
57 “common” antibiotics. Clearly, the development of ABR toward hospital antibiotics is particularly
58 dangerous, because these antibiotics are our last line of defense against ABR bacterial infections
59 (Perl, 1999; Roche et al., 2016). Resistance against antibiotics reserved for hospital settings is
60 presently limited (although it is steadily growing), either because some of these antibiotics have
61 been discovered relatively recently (which means a couple of decades ago, as no new antibiotics
62 have been discovered afterwards), or because they have undergone little general use even if known
63 by more time, due to significant side effects or relatively difficult administration (Rattie and Ravin,
64 1975; Piddock, 2011). Because of restricted prescriptions, controlled use and focus on human
65 medicine, many routes to ABR development are currently minimized for antibiotics reserved for
66 hospital settings. The same is not true for wastewater, unfortunately, because of unavoidable
67 excretion by patients of these antibiotics and of the associated resistant bacteria (Das et al., 2019;
68 Hoelle et al., 2019; Ekwanzala et al., 2020).

69 Although at the moment antibiotics are not classified as contaminants and are not regulated by law,
70 there are already some initiatives aimed at tackling the ABR issue in wastewater. Therefore, it is
71 very likely that future technological developments in WWTPs will have to achieve the removal of
72 antibiotics and other CECs from wastewater (Sharma et al., 2016; Fiorentino et al., 2018; Oberoi et
73 al., 2019; Rizzo et al., 2020). Physical separation or degradation are some of the techniques that can
74 be used to eliminate chemicals from wastewater. Among such techniques, the Fenton reaction is a
75 notable example of a potentially cost-effective treatment (Wang and Zhuan, 2020; Brillas, 2020). It
76 is an Advanced Oxidation Process based on the production of $\bullet\text{OH}$ and/or other oxidizing species

77 such as ferryl, FeO^{2+} . Classic Fenton uses soluble Fe(II) salts, and H_2O_2 usually in excess of the
78 stoichiometric ratio (Neyens et al., 2003; Mirzaei et al., 2017):



82 Classic Fenton has two major drawbacks: (i) It works best at pH 3, but its performance worsens
83 quickly as pH increases, because of slower Fe(III)-Fe(II) recycling (Pignatello et al., 2006). It is next
84 to impossible to carry out an effective treatment by classic $\text{Fe}^{2+} + \text{H}_2\text{O}_2$ under ~neutral conditions;
85 (ii) The adjustment of pH before wastewater discharge causes Fe(III) precipitation, producing a
86 sludge (Huang et al., 2013). To tackle these shortcomings, some modifications of the Fenton
87 process have been developed: (i) Photo-Fenton, where radiation facilitates the conversion of Fe(III)
88 into Fe(II) (Giannakis et al., 2018a; Giannakis et al., 2018b; Arzate et al., 2020). Unfortunately,
89 natural sunlight may not be regularly available and artificial radiation is quite costly. (ii) Use of
90 ligands to keep Fe(III) dissolved even at ~neutral pH (Wu et al., 2015; Qian et al., 2020). However,
91 there are law limits for the total dissolved Fe in wastewater (Zhong et al., 2012), and the ligands
92 may interfere with Fe elimination by precipitation. Moreover, ligands can change Fenton reactivity
93 by inducing the generation of less-reactive ferryl over $\bullet\text{OH}$, and may act as scavengers of reactive
94 species (Pignatello et al., 1999; Farinelli et al., 2020). (iii) Heterogeneous Fenton, where Fe(II) salts
95 are replaced by iron-based solid materials (Vorontsov, 2019; Tang and Wang, 2020). Research has
96 focused on magnetic or magnetizable materials because they are very easy to remove after treatment
97 (Jin et al., 2017; Gonçalves et al., 2020a; Gonçalves et al., 2020b). Among Fenton-active materials
98 with magnetic properties, micro/nanoscope zero-valent iron (Fe^0 , or ZVI) offers several advantages
99 such as availability, excellent reactivity, quite extended pH range and resistance to passivation (Joo
100 et al., 2005; Rezaei and Vione, 2018; Gil Pavas et al., 2019). For instance, compared to other
101 materials such as magnetite and titanomagnetites (Avetta et al., 2015; Bertinetti et al., 2019), ZVI

102 does not require particular storage attentions if used in the framework of the Fenton reaction, and
103 even passivated ZVI still retains significant Fenton reactivity (Minella et al., 2016).

104 The ZVI-Fenton process, alone or in combination with other techniques (*e.g.*, ultrasound or
105 radiation), has been studied for the degradation of some antibiotics, but the previously investigated
106 compounds are also widely used outside of the field of human medicine (*e.g.*, animal husbandry or
107 aquaculture). Therefore, wastewater is definitely not the unique collector of the relevant residues
108 (Perini et al., 2014; Lumbaqué et al., 2019). Degradation of antibiotics bearing halogen or nitro
109 groups has also been studied by exploiting the reductive (*i.e.*, opposite to the oxidative ones used in
110 ZVI-Fenton) capabilities of ZVI alone, without H₂O₂ (Liu et al., 2018; Xu et al., 2019; Xu et al.,
111 2020). However, in such cases, the treatment requires ZVI (or sulfide-modified ZVI) doses of
112 around 1 g L⁻¹ (Cao et al., 2017), which would be very costly in wastewater treatment applications
113 when compared with the ten-mg L⁻¹ range of ZVI in ZVI-Fenton (Minella et al., 2019).

114 To the best of our knowledge, ZVI-Fenton has never been tested with antibiotics reserved for
115 hospital settings, the elimination of which from wastewater is particularly critical. Therefore, in this
116 work we have chosen three antibiotics reserved for hospital settings, belonging to different classes
117 and having different structures (cefazolin, CFZ; imipenem, IMI, and vancomycin, VNM), to study
118 their ZVI-Fenton degradation. While antibiotics could be partially excreted as glucuronate
119 derivatives, ZVI-Fenton would be carried out after the activated sludge step, where bacteria detach
120 the sugar moiety and set free the starting compound (deconjugation) (Polesel et al., 2016).

121 In this work, we carried out ZVI-Fenton degradation in the dark of the investigated antibiotics by
122 focusing on: (*i*) optimization of ZVI and H₂O₂ doses; (*ii*) degradation efficiency at different pH
123 values; (*iii*) impact on wastewater quality (conductivity, dissolved Fe, residual H₂O₂); (*iv*) formation
124 of intermediates and, last but not least (von Gunten, 2018), (*v*) cost considerations.

125

126 **2. MATERIALS AND METHODS**

127

128 **2.1. Reagents and materials**

129 The used reagents, their manufacturers and purity grades are reported in the Supplementary
130 Material (hereinafter, **SM**), **Paragraph S1**. Commercial ZVI particles (Sigma-Aldrich, Milan, Italy,
131 purity $\geq 99.5\%$, product number 44890; <http://www.sigmaaldrich.com/catalog/product/aldrich/44890>)
132 had diameter $< 10 \mu\text{m}$. The real wastewater (WW) samples used in this work (WWa, WWb) were
133 obtained from the secondary clarifier tank outflow of two different urban WWTPs (population
134 equivalents of 51,000 and 3.9 million inhabitants, respectively). The WW samples were used after
135 rough pre-filtration with grade 1 qualitative filter paper (supplied by Whatman, Maidstone, UK), to
136 remove large suspended solids. WW characterization is described in **Paragraph S2 (SM)**, and the
137 main chemical features of the studied WW samples are reported in **Table S1 (SM)**. Note that, in
138 Italy, hospital WWTPs have been largely dismissed and hospital wastewater is currently being
139 treated together with the rest of urban wastewater, in centralized WWTPs. The disadvantage is that
140 hospital antibiotics get diluted into the general urban wastewater flow. The advantage is that
141 centralized WWTPs can afford the use of more advanced treatment technologies, and will do so in
142 the future as well. Moreover, by so doing it is also possible to intercept the fraction of antibiotics
143 that is excreted after the patients are dismissed from hospitals (prolonging hospitalization to wait for
144 excretion kinetics would be totally unrealistic because of excessive costs, and even very dangerous
145 due to increased risks of hospital infections) (Baietto et al., 2014).

146 To help quantify the amount of acid needed to fix WW pH in real wastewater treatment, WW
147 aliquots (50 mL initial volume) were titrated with a standard H_2SO_4 solution ($4.5 \times 10^{-3} \text{ mol L}^{-1}$),
148 using a potentiometric titrator (Titrino 702 SM by Metrohm, Herisau, Switzerland) equipped with a
149 Metrohm combined pH glass electrode (code number 6.0233.100), and controlled by the Metrohm
150 software "Tiamo" (titration and more).

151

152 **2.2. Degradation experiments**

153 Degradation experiments were carried out in beakers, where the reaction mixture (50 mL total
154 volume) contained ZVI, H₂O₂, the substrate (CFZ, IMI, VNM, separately or in mixture), and a
155 reagent for pH adjustment. Three experimental series were carried out: (i) separate substrates in
156 ultra-pure water; (ii) mixture (CFZ+IMI+VNM) in ultra-pure water; (iii) mixture in wastewater
157 (WWa, WWb). In the first two cases, a phosphate buffer at the desired pH value was added to the
158 reagent mixture. Unfortunately, the amount of phosphate that had to be added to keep pH constant
159 was higher than the law limits for phosphorous in WW. Therefore, in the third experimental series,
160 the pH value was fixed with H₂SO₄, which was allowed by the WW buffer capacity and would be
161 reasonable in WWTPs (Minella et al., 2019). HCl was avoided because Cl⁻ scavenges •OH in acidic
162 conditions (Jayson et al., 1973), and HNO₃ was also avoided because of toxicity and eutrophication
163 issues connected with nitrate.

164 In analogy with other studies (Méndez-Arriaga et al., 2010; Minella et al., 2018), and considering
165 that pharmaceuticals are typically found at trace levels in wastewater (CFZ and VNM have for
166 instance been detected at µg L⁻¹ level in effluents; Kümmerer and Henninger, 2003), substrate
167 concentration was kept as low as possible, but still high enough to enable reliable monitoring by
168 liquid chromatography (4-10 µmol L⁻¹, depending on the experiment).

169 At scheduled time intervals, a measured 0.9 mL sample aliquot was withdrawn from the reaction
170 mixture and added with 0.1 mL methanol, to stop the Fenton reaction (Li et al., 2010; Minella et al.,
171 2016). ZVI was then removed from the sample by filtration on Millipore Millex HV filters (0.45 µm
172 pore diameter). CFZ, IMI and VNM were quantified by high-performance liquid chromatography –
173 diode array detection (HPLC-DAD, VWR-Hitachi Elite series). Instrumental and operational details
174 are reported in **Paragraph S3 (SM)**.

175 Repeatability experiments were carried out, to assess the degree to which differences in time trends
176 can be considered as statistically significant. The results (see **Figure S1 (SM)** as an example)

177 suggest that the reproducibility of concentrations ranged between 5-20%. In these experiments, up
178 to ten samplings were carried out in each beaker, for a total withdrawal of up to 9 mL. The results
179 were compared with those of similar experiments, carried out in the same conditions but with just
180 three samplings, to limit the reduction in the volume of the reacting system. The observed
181 differences were well within the reproducibility of exactly replicated experiments.

182 The determination of dissolved (leached) iron and residual H₂O₂ was carried out with a Varian Cary
183 100 Scan double-beam UV-VIS spectrophotometer, using procedures (o-phenanthroline and
184 peroxidase/4-aminoantipyrine, respectively; Sandell, 1950; Frew et al., 1983) that are described in
185 detail in the **SM, Paragraph S3**. The spectrophotometric method used for Fe(II) and Fe(III) was
186 very suitable in this context because its detection limit (0.05 mg_{Fe} L⁻¹) was much lower than the
187 limit concentrations of Fe for wastewater discharge (1-2 mg_{Fe} L⁻¹, *vide infra*).

188 In dedicated runs, pH and conductivity of the WW samples under treatment were monitored over
189 time by using, respectively, a 98100 Checker pH meter and a HI2030 Multi-parameter probe, both
190 by Hanna Instruments (Rhode Island, USA).

191

192 **2.3. Electron Paramagnetic Resonance (EPR) measurements**

193 The reaction systems containing ZVI + H₂O₂ were added with the spin trap 5,5-dimethyl-1-
194 pyrrolidine-N-oxide (DMPO). Sample aliquots (50 μL) were taken at scheduled time intervals from
195 the reaction mixtures using a capillary glass tube, which was sealed with plasticine on the one end
196 and inserted into the EPR cavity. The instrument used was a Miniscope 100 EPR Spectrometer
197 (Magnettech, Berlin, Germany). The operational parameters were as follows: middle of the range
198 3345 G, scan range 120 G, modulation amplitude 1000 mG, attenuation 7 dB, time 60 s, gain value
199 3, phase 180. The target was to identify the DMPO-OH adduct.

200

201 **2.4. Identification of degradation intermediates**

202 In this series of experiments the concentration of each antibiotic (2×10^{-4} mol L⁻¹) was higher than
203 in the degradation runs, to make the identification of the intermediates easier. Wastewater was not
204 used here, to avoid possible interaction or matrix effects that could complicate the interpretation of
205 chemical structures. At scheduled reaction times, aliquots of 0.80 mL of the reacted solution were
206 withdrawn and subjected to analysis by ultra-high performance liquid chromatography-tandem mass
207 spectrometry (UHPLC-MS/MS, Nexera Shimadzu, Kyoto, Japan), after the addition of 0.20 mL of
208 methanol and filtration on 0.2 µm PTFE filters (VWR International, Darmstadt, Germany). See **SM,**
209 **Paragraph S3** for details of the UHPLC-MS/MS measurements.

210

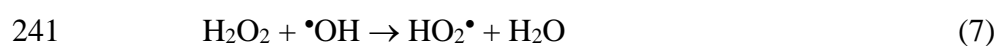
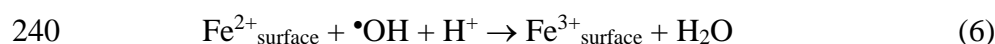
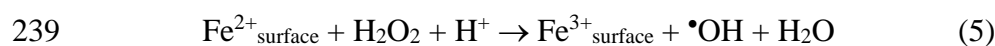
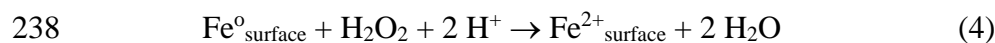
211 **3. RESULTS AND DISCUSSION**

212

213 **3.1. Preliminary experiments of antibiotics degradation in ultra-pure water**

214 A first series of experiments was carried out in ultra-pure water to check for the ability of ZVI-
215 Fenton to degrade the three studied compounds, taken separately, under the most favorable
216 conditions (absence of wastewater interfering agents). Coherently with previous findings (Minella
217 et al., 2016; Minella et al., 2019) the ZVI-Fenton system worked best at pH 3, and performance
218 gradually decreased (but was by no means totally lost) with increasing pH, in keeping with the fact
219 that the \bullet OH yield of the Fenton reaction decreases with increasing pH (Farinelli et al., 2020).
220 Actually, it was possible to offset the reactivity loss by increasing both H₂O₂ concentration and ZVI
221 loading, obtaining complete or almost complete degradation also at pH 6 or 7. Compared to pH 3, it
222 was necessary to increase the H₂O₂ concentration by 4-8 times, and the ZVI loading by 2-3 times to
223 obtain effective degradation at pH 6-7 (see **Figures S2, S3 (SM)**). Note that the added costs linked
224 with the dose increase would not hamper the economics of the process significantly (*vide infra*).

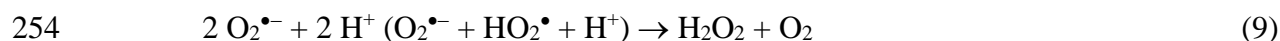
225 Most of the generation of $\bullet\text{OH}$ (and/or other oxidizing species) in the ZVI-Fenton process stems
226 from direct interaction between H_2O_2 and the ZVI surface, while the detected values of dissolved
227 Fe(II, III) are very low and allow for excluding a significant role of the homogeneous-phase process
228 (Minella et al., 2016 & 2019). The reasonable reactions involved in the heterogeneous process
229 would take place between H_2O_2 and surface Fe^0 or Fe(II) species. Fe(II) species are likely to already
230 occur on the ZVI surface from the very start (*e.g.*, due to storage of ZVI in air), especially in the
231 absence of acid-washing treatments to remove them. While decreasing the ZVI reactivity in general,
232 surface Fe(II) can be involved in the Fenton reaction and would thus not be a problem in this
233 context. Because the reaction involves $\text{ZVI} + \text{H}_2\text{O}_2$, by increasing the ZVI loading and/or the H_2O_2
234 concentration one could offset the decreasing production yield of $\bullet\text{OH}$ as the pH increases, although
235 only up to a certain degree. Actually, a further increase of ZVI and/or H_2O_2 beyond the optimum
236 values would decrease the degradation efficiency, as both reactants can scavenge $\bullet\text{OH}$ as well as
237 contribute to its production (Minella et al., 2019):



242 Because satisfactory results are hardly achieved with the classic or modified Fenton reaction at
243 \sim neutral pH (in which case reactivity is often totally lost; Jung et al., 2009), the ability of ZVI-
244 Fenton to still work well in \sim neutral conditions makes it very attractive for water treatment.

245 IMI undergoes rather fast hydrolysis at pH 4 or lower. Therefore, the ZVI-Fenton degradation of
246 IMI was only tested in the pH range 5-7 (**Figure S4 (SM)**), where hydrolysis is slow enough to be
247 negligible at the experimental time scales. Significant hydrolysis of CFZ and VNM could be
248 excluded at all the investigated pH values.

249 Some removal of the three studied compounds was also achieved in the presence of ZVI alone,
250 without H₂O₂ (blank experiments; **Figures S2-S4 (SM)**). Part of the reason could be the adsorption
251 of the substrates on ZVI, but this material is also known to trigger the Fenton reaction in the
252 presence of dissolved O₂ (reactions 8-10) (Joo et al., 2005):



256 However, antibiotic removal by ZVI alone was considerably less effective compared to ZVI + H₂O₂
257 (**Figures S2-S4 (SM)**), even when taking into account the experimental variability (**Figure S1**
258 **(SM)**). Indeed, the addition of H₂O₂ was strictly required to achieve complete removal of the
259 contaminants in 1 h. The Fenton-like reaction ZVI + H₂O₂ is considerably more effective than ZVI
260 adsorption and/or the process involving ZVI + O₂, where H₂O₂ is generated in rather small amounts
261 by O₂^{•-}/HO₂[•] dismutation (Keenan and Sedlak, 2008). Moreover, the three antibiotics did not
262 undergo degradation in the presence of H₂O₂ alone, without ZVI (data not shown).

263 To avoid IMI hydrolysis, the degradation of the three antibiotics in mixture was studied at pH 5-7.
264 The three compounds taken separately underwent effective degradation under similar but not
265 identical conditions. Actually, it was not possible to find conditions similar to those ensuring
266 degradation of the separate compounds, under which the compounds in mixture could be degraded
267 efficiently (see **Table S3 (SM)** for a summary of these preliminary experiments, where the doses of
268 ZVI and H₂O₂ were varied). A possible solution to this problem is to make the reaction conditions
269 more stringent, *e.g.*, by increasing the concentration of H₂O₂. However, ZVI and H₂O₂ behave as
270 scavengers of •OH and other oxidizing reactive species, in addition to producing them (Buxton et
271 al., 1988). Therefore, both ZVI and H₂O₂ have optimal doses for degradation, and a further increase
272 above a certain limit is actually detrimental (Minella et al., 2019). As an alternative, reagents can be
273 added multiple times. In the case of H₂O₂, which is degraded over time under Fenton conditions
274 (*vide infra*), multiple additions ensure sufficiently high but not excessive concentrations at any time

275 point, thereby limiting the role of H₂O₂ as scavenger (Minella et al., 2018). Very satisfactory
276 performance was achieved by adding H₂O₂ both at the start of the reaction, and a second time after
277 30 min (see arrows in **Figure 1**). The addition at 30 min consisted in a very small amount of a
278 concentrated H₂O₂ solution (5 or 10 μL depending on the pH value, 1 mol L⁻¹), not to significantly
279 alter the overall volume of the reaction mixture. By so doing, complete or almost complete
280 degradation of CFZ, IMI and VNM was achieved in one hour at pH 5-7 with ZVI + H₂O₂, while
281 ZVI alone was much less effective (**Figure 1**). It was necessary to offset the decrease in Fenton
282 reactivity with increasing pH by progressively increasing the initial/added H₂O₂ concentration
283 and/or ZVI loading, at the same time avoiding the use of excessive amounts of either species.

284 A possible reason for the significant ZVI-Fenton reactivity under near-neutral conditions, which
285 differentiates ZVI-Fenton from classic, homogeneous Fenton is that the latter relies on Fe(III)-
286 Fe(II) recycling, which is hampered by Fe(III) precipitation at near-neutral pH. An additional
287 reason could be a different reaction mechanism. Indeed, homogeneous Fenton yields significant
288 amounts of •OH at pH 2-3 (•OH yield ~60%; Minero et al., 2013), but the production of •OH
289 decreases significantly as the pH increases. Ferryl (FeO²⁺) replaces •OH as the Fenton oxidant at
290 near-neutral pH (Farinelli et al., 2020), and the lower reactivity of FeO²⁺ compared to •OH might
291 contribute to the decrease in Fenton degradation performance. Our EPR measurements showed that
292 •OH (identified as the DMPO-OH adduct) still occurred significantly with ZVI-Fenton at pH 6 (see
293 **Figure S5a (SM)**). A •OH-based reactivity in near-neutral pH conditions would be consistent with
294 the significant degradation of antibiotics observed with ZVI-Fenton at pH 5-7. Moreover, the
295 generation of the Fenton oxidant would likely involve a reaction between H₂O₂ and the ZVI surface,
296 as suggested by previous results (Minella et al., 2016), while aqueous Fe species played little to
297 negligible role in •OH generation (see **Figure S5b (SM)**). This finding agrees well with the
298 negligible levels of leached Fe that were detected in the studied reaction systems (*vide infra*).

299

300 **3.2. ZVI-Fenton degradation of antibiotics in partially treated wastewater**

301 The ZVI-Fenton degradation was then carried out in wastewater matrix (the two wastewater
302 samples WWa and WWb had different characteristics, see **Table S1 (SM)**), spiked with a mixture
303 of CFZ, IMI and VNM, each at $4 \mu\text{mol L}^{-1}$ initial concentration.

304 Wastewater contains several organic and inorganic interfering compounds that inhibit the Fenton
305 reaction (Salgota et al., 2006; Zhang et al., 2019; Ricceri et al., 2019). Therefore, compared to ultra-
306 pure water, it is necessary to increase the doses of ZVI and H_2O_2 to still achieve effective
307 degradation in wastewater. Multiple additions of reagents are often a compulsory choice to
308 minimize the scavenging of reactive transient species by ZVI and H_2O_2 (Minella et al., 2018;
309 Minella et al., 2019). Many optimization experiments were carried out to look for suitable
310 degradation conditions, which returned the following key indications: (i) Almost negligible
311 abatement of the studied antibiotics was observed with ZVI alone; therefore, significant adsorption
312 on ZVI or degradation by $\text{ZVI} + \text{O}_2$ can be practically excluded in secondary wastewater. (ii)
313 Effective degradation was achieved at pH 5 but not at pH 6 or 7 (see for instance **Figure S6** and
314 **Table S4 (SM)** for a summary of the experiments carried out at pH 6, varying the H_2O_2 and ZVI
315 doses within the framework of multiple additions); from this point of view, CFZ, IMI and VNM
316 look more recalcitrant to ZVI-Fenton degradation compared to, *e.g.*, ibuprofen (Minella et al.,
317 2019). (iii) Complete degradation in wastewater required 90 min reaction time, as compared to 60
318 min in ultra-pure water. (iv) The pH value tended to increase during the reaction (possibly due to
319 H^+ -consuming processes, such as (4)-(6)), and it was thus necessary to monitor and correct it by a
320 small addition of acid as the reaction progressed. For instance, in both WWa and WWb at initial pH
321 5, it was necessary to adjust pH back to 5 at 30 min reaction time, to offset gradual pH increase and
322 achieve satisfactory degradation. The pH of the two systems (WWa, WWb) continued increasing
323 after 30 min to reach a final value of 5.7-5.8 at 90 min, which is suitable for wastewater discharge
324 ($5.5 \leq \text{pH} \leq 9.5$) (Barbagallo et al., 2001). For this reason, and because effective degradation could
325 be achieved anyway, after 30 min the pH was monitored but no longer corrected. The time trends of

326 CFZ, IMI and VNM at pH 5 are reported in **Figure 2**, for WWa (**2a**) and WWb (**2b**). The
327 conditions reported in the figure are those allowing for the best degradation with the lowest
328 consumption of reagents.

329 Conductivity is an important parameter for wastewater quality, because saline wastewaters are less
330 suitable for discharge or, most notably, reuse in agriculture (Hussain et al., 1999). Treatments
331 requiring pH adjustment may affect conductivity, thus the time trends of conductivity were
332 monitored. The results observed in both wastewaters (WWa, WWb) are reported in **Figure S8**
333 (**SM**). A very slight conductivity increase was observed, presumably because of SO_4^{2-} addition.
334 However, conductivity changes were quite small and would not affect the wastewater requirements
335 for discharge or reuse, even in the demanding field of agriculture (Salgota et al., 2006).

336 The ZVI-Fenton treatment relies on H_2O_2 addition, and in some contexts, the elimination of H_2O_2
337 after treatment might be an issue (in other cases, residual H_2O_2 may be welcome as a disinfectant)
338 (Bownik and Stepniewska, 2015). For this reason, the time trend of H_2O_2 under ZVI-Fenton was
339 studied (see **Figure S9 (SM)**). Interestingly, H_2O_2 underwent consistent degradation despite
340 additions at 30 and 60 min, and H_2O_2 was negligible in solution at the end of the reaction (90 min).
341 Therefore, the post-treatment elimination of H_2O_2 would not be necessary.

342 Dissolved Fe (either Fe(II) or Fe(III)) was monitored during the ZVI-Fenton reaction at pH 5 and 6,
343 but it was always undetectable ($< 0.05 \text{ mg}_{\text{Fe}} \text{ L}^{-1}$; data not shown). This finding excludes significant
344 Fe leaching from ZVI to the aqueous solution (as an alternative, there could be leaching followed
345 by fast precipitation on the solid). Actually, dissolved Fe is not necessary for the ZVI-Fenton
346 system to work, because the process can be triggered by the reaction of the iron sites at the ZVI
347 surface with dissolved H_2O_2 (a genuine heterogeneous Fenton process) (Minella et al., 2016). The
348 lack of dissolved Fe is very positive when considering the maximum Fe levels allowed by
349 legislation in many countries ($1 \text{ or } 2 \text{ mg}_{\text{Fe}} \text{ L}^{-1}$) (Barbagallo et al., 2001; Salgota et al., 2006; Zhong
350 et al., 2012; National Environmental Agency, 2016).

351 To sum up, the optimized operational conditions for the effective degradation of CFZ, IMI and
352 VNM (initial pH 5) are reported in **Table S5 (SM)**. They are the same for both WWa and WWb.

353

354 **3.3. Identification of degradation intermediates**

355 An MS/MS characterization study was first performed upon infusion into the mass spectrometer of
356 methanolic standard solutions of each antibiotic at $100 \mu\text{g L}^{-1}$, in order to find the most abundant
357 product ions and the fragmentation pathways, which could be useful to identify the chemical
358 structures of the intermediates. All the analytes were ionized in both positive and negative ion
359 modes, but the first was the most sensitive and was selected for further runs. **Figures S10 - S12**
360 **(SM)** show the MS/MS spectra of CFZ, IMI and VNM, respectively.

361 Eighteen intermediates for CFZ, five for IMI and three for VNM were identified by UHPLC-
362 MS/MS. An additional six compounds were detected for VNM, but they were likely synthesis
363 impurities that already occurred at $t = 0$. Indeed, their abundance decreased as the reaction
364 progressed. Chemical structures are proposed on the basis of MS spectra, isotopic cluster obtained
365 by Enhanced Resolution experiments, and interpretation of MS/MS product ions. All the proposed
366 structures gave 95-100% matching compared to *in silico* fragmentation. A tentative reaction scheme
367 is reported in **Scheme 1** (more comprehensive structural data including the main fragments are
368 reported in **Table S6 (SM)**).

369 Eighteen CFZ intermediates were identified, many of which are structural isomers (the relevant
370 MS/MS spectra are reported in **Figures S13 – S30 (SM)**). Many chemical structures showed
371 opening (CFZ-P5c, CFZ-P5d, CFZ-P6a, CFZ-P6b), loss (CFZ-P3 and CFZ-P7) or modification
372 (CFZ-P1a, CFZ-P1b, CFZ-P1c, CFZ-P5a, CFZ-P5b) of the beta-lactam ring. CFZ-P4a and CFZ-
373 P4b were the intermediates with the highest peak areas and were identified as sulfoxide compounds,
374 in which thioether oxidation occurred at two different S atoms. The chemical structures of these two
375 compounds have been already reported upon oxidation of CFZ by KMnO_4 (Li et al., 2016).

376 Sulfoxide groups also occur in the proposed structures of CFZ-P1a, CFZ-P1b and CFZ-P1c, where
377 the formation of an aziridine ring would follow the loss of formaldehyde from the beta-lactam ring.
378 CFZ-P5 showed two couples of sulfoxide-containing isomers: the first had an aziridine ring (CFZ-
379 P5a and CFZ-P5b), the second was characterized by beta-lactam ring-opening (CFZ-P5c and CFZ-
380 P5d). CFZ-P6a and CFZ-P6b were the hydroxylated forms of CFZ-P5c and CFZ-P5d, respectively.
381 CFZ-P7 had the same chemical structure as CFZ-P1a, except for the formation of sulfoxide.
382 The proposed chemical structures of CFZ-P2a and CFZ-P2b are characterized by tetrazole loss and
383 cleavage of the dihydrothiazine ring. The structure of CFZ-P3b (already present at trace level as
384 CFZ impurity, and showing intensity increase during the degradation) corresponds to 5-methyl-4,5-
385 dihydro-1,3,4-thiadiazole-2-thiol, as previously reported in the photocatalytic degradation of CFZ
386 (Gurkan et al., 2012). In contrast, a linear structure compatible with the MS/MS fragmentation
387 spectrum is proposed for CFZ-P3a. Finally, CFZ-P8a and CFZ-P8b were characterized by the loss
388 of the thiadiazole group.

389 Five degradation intermediates were detected for IMI (see **Figures S31 – S35 (SM)** for their
390 MS/MS spectra), among which IMI-P1 was already present at $t = 0$ and rapidly increased after 5
391 min reaction time, quickly becoming the most intense intermediate of IMI. The proposed structure
392 is 3-(methylsulfanyl)-1H-pyrrole-2-carboxylic acid. IMI-P2, IMI-P3 and IMI-P4 were also present
393 in traces at $t = 0$, probably due to IMI instability (De Souza Barbosa et al., 2019), and increased
394 afterwards. IMI-P2 showed the opening of the beta-lactam ring, as already found in the metabolic
395 degradation of IMI (Abdel-Moety et al., 2010), whereas IMI-P3, IMI-P4 and IMI-P5 were formed
396 by reaction of the IMI diazene moiety to produce carboxylic and oxoacetic acids.

397 The chemical structure of VNM is very complex and includes an aminoglycoside and a polypeptide
398 moiety. Direct infusion showed that the product ions at m/z 100, 118 and 144 were formed by
399 fragmentation of the aminoglycoside moiety, which is important for the interpretation of the
400 structures of the intermediates. Indeed, the latter preserved the aminoglycoside moiety, while
401 degradation usually occurred on the polypeptide one.

402 The MS/MS spectra of the three detected VNM intermediates are shown in **Figures S36 – S38**
403 **(SM)**. VNM-P1 corresponds to $[M-OH+H]^{2+}$ at m/z 715.6, VNM-P2 (m/z 730.7) derives from
404 CH_3N loss and N-acetylation, VNM-P3 (m/z 731.2) derives from water loss, oxidation and further
405 methylation. The structures of VNM-P2 and VNM-P3 have been proposed as intermediates of
406 VNM degradation in the environment (Cao et al., 2018). Other species were found at $t = 0$ (VNM-
407 P4a, VNM-P4b, VNM-P5a, VNM-P5b, VNM-P6a, and VNM-P6b; **Figures S39 – S43 (SM)**), more
408 likely as synthesis impurities rather than degradation intermediates (Hadwiger et al., 2012; Belissa
409 et al., 2014; Cao et al., 2018). Indeed, their signal intensities decreased during the reaction.

410 The intermediates that potentially pose the highest concern are those with antibiotic properties,
411 which could still promote the development of ABR and/or the selection of antibiotic-resistant
412 bacteria. The antibiotic action of VNM stems from rather complex interactions (Ndieyira et al.,
413 2017), the modification of which upon structural changes is poorly predictable. In contrast, the CFZ
414 and IMI intermediates that might still act as antibiotics are those having an intact β -lactam ring
415 (Takata et al., 1981; Wright et al., 2017). They are CFZ-P4a,b, as well as IMI-P3, IMI-P4 and IMI-
416 P5.

417 The chromatographic peak areas give some tentative insight into the compounds abundance: the
418 time trends of the peak areas of the primary antibiotic, the antibiotic plus the lactam ring-retaining
419 intermediates, and the antibiotic plus all the intermediates are reported in **Figure S44a** (CFZ) and
420 **S44b** (IMI) of the SM. The chromatographic peak areas of the primary antibiotics strongly prevail
421 over those of the ring-retaining intermediates and, additionally, the latter would account for a small
422 fraction of degraded CFZ and a negligible fraction of degraded IMI. Therefore, it can be assumed
423 that when all the primary antibiotic has disappeared, as observed in the degradation experiments of
424 **Section 3.2**, the anti-microbial action of the degraded mixture would be only a very small fraction
425 of the initial one.

426

427 **3.4. Approximate estimate of treatment costs**

428 The optimized reaction conditions for wastewater reported in **Table S5 (SM)** were the basis for a
429 preliminary cost assessment, scaling the total added amounts of ZVI, H₂O₂ and acid from the
430 laboratory volume (50 mL) to 1 m³ wastewater. Both the acid amount needed to fix the initial pH
431 value and that used to adjust pH during the reaction were taken into account. Furthermore, there
432 would be no need to add a base to adjust pH at the end of the treatment, because the final pH value
433 was 5.7-5.8. Only the overall costs of the reactants are considered at this stage, thereby neglecting
434 other costs such as investment costs, energy and human labor. This approach yields a lower limit for
435 the actual costs, but chemicals are usually the main expenditure in Fenton treatments (Balabanič et
436 al., 2012). Current commercial costs of bulk chemicals were thus considered (Made-in-china.com,
437 2020), and the results are reported in **Table 1**. These costs would be added to those of traditional
438 wastewater treatment (around 0.38 \$ m⁻³) (Minella et al., 2018), and they differ between WWa and
439 WWb due to the different amounts of H₂SO₄ that were needed to fix pH. The reason is that WWa
440 had lower alkalinity compared to WWb (**Table S1 (SM)**).

441 The addition of a tertiary treatment step based on ZVI-Fenton would increase the overall treatment
442 costs by merely 9-17%, depending on the wastewater type, but it would ensure the degradation of
443 compounds that the traditional treatment does not remove. These compounds are not limited to
444 antibiotics reserved for hospital settings, because the same or very similar conditions are known to
445 induce the degradation of other contaminants of emerging concern such as ibuprofen (Minella et al.,
446 2019).

447 The ZVI-Fenton costs (**Table 1**) look very competitive, although successful operation at pH 5
448 requires higher doses of H₂O₂ and ZVI compared to, e.g., pH 3: costs are comparable with those of
449 UV treatment intended for disinfection (which is much cheaper compared to UV for depolluting, as
450 the latter needs higher irradiance and longer contact times), and they are quite lower than ozonation
451 costs (Dore et al., 2020). As a further comparison, ZVI alone used as reductant at a dose of 1 g L⁻¹

452 for the dehalogenation of halogen-containing antibiotics (Cao et al., 2017) would cost about 0.8 \$
453 m⁻³, which could be an important economic burden in the field of wastewater treatment.

454

455 **3.5. Implications for wastewater treatment**

456 The ZVI-Fenton technique would not work at the natural pH of wastewater (7.5-7.8 in the present
457 case), but the treatment methods that are based on pH adjustment (in the present case, acidification
458 + neutralization) have the potential to adversely affect the conductivity of the water matrix.
459 However, differently from classic Fenton that requires strongly acidic conditions, the present results
460 show that the additions of H₂SO₄, needed to fix the initial pH to 5 and to maintain it during the
461 reaction, would affect conductivity to an insignificant degree. Therefore, the ZVI-Fenton treatment
462 step would not hamper even the demanding reuse of wastewater in agriculture, provided that initial
463 wastewater conductivity meets the relevant guidelines. The reason is that pH 5 is still sufficiently
464 near neutrality to limit the added amount of H₂SO₄, which benefits both process economics and
465 treated effluent conductivity. This is a considerable advantage of ZVI-Fenton over traditional
466 Fenton, which needs to be operated at pH 3 or near 3 to achieve effective degradation in the
467 wastewater matrix (Minella et al., 2018).

468 Another important advantage of ZVI-Fenton over other Fenton-based techniques is that H₂O₂ reacts
469 at the solid surface, with no need for dissolved Fe(II) species to trigger the reaction. Therefore,
470 degradation is effective even in the presence of undetectable dissolved Fe, which cancels the need
471 for a final step of dissolved Fe precipitation and sedimentation. There would still be the need to
472 remove ZVI after treatment, but the procedure would be highly simplified by its magnetic
473 properties. The lack of residual H₂O₂ after treatment might or might not be a positive issue in view
474 of final disinfection (preliminary experiments suggest that such an additional step would be
475 required, data not shown). However, unless H₂O₂ itself is used later to disinfect wastewater, the
476 occurrence of residual H₂O₂ in solution would be more of a problem, because of possible unwanted
477 interactions with other disinfectants such as HClO (Shams El Din and Mohammed, 1998).

478 Therefore, the lack of residual H₂O₂ after ZVI-Fenton would be a positive occurrence in most cases,
479 and make a later step of H₂O₂ elimination unnecessary.

480 The scaling up of the ZVI-Fenton treatment from the lab size to an urban WWTP would certainly
481 be challenging. Experiments were here made in batch mode, which in full-scale conditions would
482 require a very large tank or even a series of large tanks, where stirring of the ZVI solid might be an
483 issue. A flow-through system might be an interesting alternative, but studies on how such a system
484 might be designed or conducted are currently lacking. Therefore, further research is still needed to
485 understand which configuration is more likely to work under full-scale conditions.

486 The ZVI-Fenton step should ideally be located after secondary treatment (activated sludge process)
487 and before the phosphorous elimination step. Such a step should also involve magnetic ZVI
488 precipitation if the process is run in batch mode, which might aid the recovery by traditional
489 precipitation of P-containing compounds such as struvite. In this way, the ZVI-Fenton step might
490 positively interact with the recovery of added-value products from wastewater. In contrast, ZVI
491 precipitation might not be needed in the case of a flow-through design, the detailed features of
492 which should, however, still be defined.

493

494 **4. CONCLUSIONS**

495

496 This work shows that ZVI-Fenton can achieve effective and cheap elimination of antibiotics
497 reserved for hospital settings, thereby giving a potentially important contribution to fight the onset
498 of bacterial resistance against these life-saving and last-resort drugs. The identified transformation
499 intermediates of the studied antibiotics (CFZ, IMI and VNM) indeed suggest that, once the primary
500 contaminant is eliminated, most of the potential to trigger ABR is removed. In actual wastewater
501 the process is effective at pH 5, with a very limited impact of acidification on treatment costs or
502 wastewater conductivity, even in the case of wastewater reuse in agriculture. The absence of Fe

503 leaching from ZVI is positive for wastewater quality and, compared to other Fenton techniques,
504 elimination after treatment of magnetic ZVI would be much easier than removal of dissolved Fe or
505 Fe sludge. Finally, the same conditions would be effective towards other contaminants of emerging
506 concern, including recalcitrant pharmaceuticals (Minella et al., 2019), thereby anticipating future
507 wastewater legislation (Brack et al., 2015).

508

509 **ACKNOWLEDGEMENTS**

510 DV acknowledges financial support by Università di Torino and Compagnia di San Paolo (project
511 “Abatement of pharmaceuticals in hospital wastes - ABATEPHARM”), which also provided
512 funding for FF’s bursary. RS, ADC and GC acknowledge financial support by the project “Novel
513 wastewater disinfection treatments to mitigate the spread of antibiotic resistance in agriculture -
514 WARFARE”, financed by Fondazione Cariplo. We would like to thank the staff of Acqua
515 Novara.VCO S.p.A. for providing wastewater samples.

516

517 **References**

518

519 Abdel-Moety, E. M., Elragehy, N. A., Hassan, N. Y., Rezk, M. R., 2010. Selective determination of
520 ertapenem and imipenem in the presence of their degradants. *J. Chromatogr. Sci.* 48, 624-630.

521 Ahmed, M. B., Zhou, J. L., Ngo, H. H., Guo, W., Thomaidis, N. S., Xu, J., 2017. Progress in the
522 biological and chemical treatment technologies foremerging contaminant removal from
523 wastewater: A critical review. *J. Hazard. Mater.* 323, 274-298.

524 Amador, P. P., Fernandes, R. M., Prudêncio, M. C., Barreto, M. P., Duarte, I. M., 2015. Antibiotic
525 resistance in wastewater: occurrence and fate of Enterobacteriaceae producers of class A and
526 class C β -lactamases. *J. Environ. Sci. Health A – Tox. Hazard. Subst. Environ. Eng.* 50, 26-
527 39.

528 Arzate, S., Campos-Mañas, M. C., Miralles-Cuevas, S., Agüera, A., García Sánchez, J. L., Sánchez
529 Pérez, J. A., 2020. Removal of contaminants of emerging concern by continuous flow solar
530 photo-Fenton process at neutral pH in open reactors. *J. Environ. Manage.* 261, 110265.

531 Avetta, P., Pensato, A., Minella, M., Malandrino, M., Maurino, V., Minero, C., Hanna, K., Vione,
532 D., 2015. Activation of persulfate by irradiated magnetite: implications for the degradation
533 of phenol under heterogeneous photo-Fenton-like conditions. *Environ. Sci. Technol.* 49,
534 1043-1050.

535 Baietto, L., Corcione, S., Pacini, G., Di Perri, G., D'Avolio, A., De Rosa, F. G., 2014. A 30-years
536 review on pharmacokinetics of antibiotics: Is the right time for pharmacogenesis? *Curr.*
537 *Drug Metab.* 15, 581-598.

538 Balabanič, D., Hermosilla, D., Merayo, N., Krivograd Klemenčič, A., Blanco, A., 2012.
539 Comparison of different wastewater treatments for removal of selected endocrine-disruptors
540 from paper mill wastewaters. *J. Environ. Sci. Health A* 47, 1350–1363.

541 Barbagallo, S., Cirelli, G. L., Indelicato, S., 2001. Wastewater reuse in Italy. *Water Sci. Technol.*
542 43, 43-50.

543 Behera, S. K., Kim, H. W., Oh, J.-E., Park, H.-S., 2011. Occurrence and removal of antibiotics,
544 hormones and several other pharmaceuticals in wastewater treatment plants of the largest
545 industrial city of Korea. *Sci. Total Environ.* 409, 4351-4360.

546 Belissa, E., Nino, C., Bernard, M., Henriët, T., Sadou-Yaye, H., Surget, E., Boccadifuoco, G.,
547 Yagoubi, N., Do, B., 2014. Liquid chromatography–tandem mass spectrometry for
548 simultaneous determination of ticarcillin and vancomycin in presence of degradation products.
549 Application to the chemical stability monitoring of ticarcillin - vancomycin solutions. *J.*
550 *Chromatogr. Sep. Tech.* 5, 5.

551 Bengtsson-Palme, J., Larsson, D. G. J., 2016. Concentrations of antibiotics predicted to select for
552 resistant bacteria: Proposed limits for environmental regulation. *Environ. Internat.* 86, 140-
553 149.

554 Bertinetti, S., Hanna, K., Minella, M., Minero, C., Vione, D., 2019. Fenton-type processes triggered
555 by titanomagnetite for the degradation of phenol as model pollutant. *Desal. Water Treat.*
556 151, 117-127.

557 Bownik, A., Stepniewska, Z., 2015. Protective effects of ectoine on behavioral, physiological and
558 biochemical parameters of *Daphnia magna* subjected to hydrogen peroxide. *Comp.*
559 *Biochem. Physiol. C Toxicol. Pharmacol.* 170, 38-49.

560 Brack, .W., Altenburger, R., Schüürmann, G., Krauss, M., López Herráez, D., van Gils, J.,
561 Slobodnik, J., Munthe, J., Gawlik, B. M., van Wezel, A., Schriks, M., Hollender, J.,
562 Tollefsen, K. E., Mekenyan, O., Dimitrov, S., Bunke, D., Cousins, I., Posthuma, L., van den
563 Brink, P. J., López de Alda, M., Barceló, D., Faust, M., Kortenkamp, A., Scrimshaw, M.,
564 Ignatova, S., Engelen, G., Massmann, G., Lemkine. G., Teodorovic. I., Walz, K. H., Dulio,
565 V., Jonker, M. T., Jäger, F., Chipman, K., Falciani, F., Liska, I., Rooke, D., Zhang, X.,
566 Hollert, H., Vrana, B., Hilscherova, K., Kramer, K., Neumann, S., Hammerbacher, R.,
567 Backhaus, T., Mack, J., Segner, H., Escher, B., de Aragão Umbuzeiro, G., 2015. The
568 SOLUTIONS project: challenges and responses for present and future emerging pollutants
569 in land and water resources management. *Sci. Total Environ.* 503-504, 22-31.

570 Brillas, E., 2020. A review on the photoelectro-Fenton process as efficient electrochemical
571 advanced oxidation for wastewater remediation. Treatment with UV light, sunlight, and
572 coupling with conventional and other photo-assisted advanced technologies. *Chemosphere*
573 250, 126198.

574 Buxton, G. V., Greenstock, C. L., Helman, W. P., Ross, A. B., 1988. Critical review of rate
575 constants for reactions of hydrated electrons, hydrogen atoms and hydroxyl radicals
576 ($\bullet\text{OH}/\bullet\text{O}^-$) in aqueous solution. *J. Phys. Chem. Ref. Data* 17, 513–886.

577 Cao, Z., Liu, X., Xu, J., Zhang, J., Yang, Y., Zhou, J., Xinhua Xu, X., Lowry, G. V., 2017. Removal
578 of antibiotic florfenicol by sulfide-modified nanoscale Zero-Valent Iron. *Environ. Sci.*
579 *Technol.* 51, 11269–11277.

580 Cao, M., Feng, Y., Zhang, Y., Kang, W., Lian, K., Ai, L., 2018. Studies on the metabolism and
581 degradation of vancomycin in simulated in vitro and aquatic environment by UHPLC-Triple-
582 TOF-MS/MS. *Sci. Rep.* 8, 15471.

583 Cars, O., 2014. Securing access to effective antibiotics for current and future generations. Whose
584 responsibility? *Uppsala J. Med. Sci.* 119, 209-214.

585 Cox, J.A.G., 2017. Worthington, T. The ‘Antibiotic Apocalypse’ – Scaremongering or scientific
586 reporting? *Trends Microbiol.* 25, 167-169.

587 Cully, M., 2014. Public health: The politics of antibiotics. *Nature* 509, S16.

588 Das, N., Madhavan, J., Selvi, A., Das, D., 2019. An overview of cephalosporin antibiotics as
589 emerging contaminants: A serious environmental concern. *3 Biotech.* 9, 231.

590 De Souza Barbosa, F., Capra Pezzi, L., Tsao, M., Franco de Oliveira, T., Manoela Dias Macedo, S.,
591 Schapoval E. E. S., Mendez, A. S. L., 2019. Stability and degradation products of imipenem
592 applying high-resolution mass spectrometry: An analytical study focused on solutions for
593 infusion. *Biomed. Chromatogr.* 33, e4471.

594 Di Cesare, A., Fontaneto, D., Doppelbauer, J., Corno, G., 2016. Fitness and recovery of bacterial
595 communities and antibiotic resistance genes in urban wastewaters exposed to classical
596 disinfection treatments. *Environ. Sci. Technol.* 50, 10153-10161.

597 Dore, M. H. I., Khaleghi-Moghadam, A., Singh, R. G., Achari, G., 2020. Costs and the choice of
598 drinking water treatment technology in small and rural systems.
599 <https://ww.gov.nl.ca/mae/files/waterres-training-adww-decade-05-mohammed.dore.pdf>, last
600 accessed June 2020.

601 Ekwanzala, M. D., Dewar, J. B., Kamika, I., Momba, M. N., 2020. Comparative genomics of
602 vancomycin-resistant *Enterococcus* spp. revealed common resistome determinants from
603 hospital wastewater to aquatic environments. *Sci Total Environ.* 719, 137275.

604 Farinelli, G., Minella, M., Pazzi, M., Giannakis, S., Pulgarin, C., Vione, D., Tiraferri, A., 2020.
605 Natural iron ligands promote a metal-based oxidation mechanism for the Fenton reaction in
606 water environments. *J. Hazard. Mater.* 393, 122413.

607 Fiorentino, A., Cucciniello, R., Di Cesare, A., Fontaneto, D., Prete, P., Rizzo, L., Corno, G., Proto,
608 A., 2018. Disinfection of urban wastewater by a new photo-Fenton like process using Cu-
609 iminodisuccinic acid complex as catalyst at neutral pH. *Water Res.* 146, 206-215.

610 Frew, J. E., Jones, P., Scholes, G., 1983. Spectrophotometric determination of hydrogen peroxide
611 and organic hydroperoxides at low concentrations in aqueous solution. *Anal. Chim. Acta* 155,
612 139–150.

613 Giannakis, S., Le, T. M., Entenza, J. M., Pulgarin, C., 2018a. Solar photo-Fenton disinfection of 11
614 antibiotic-resistant bacteria (ARB) and elimination of representative AR genes. Evidence
615 that antibiotic resistance does not imply resistance to oxidative treatment. *Water Res.* 143,
616 334-345.

617 Giannakis, S., Voumard, M., Rtimi, S., Pulgarin, C., 2018b. Bacterial disinfection by the photo-
618 Fenton process: Extracellular oxidation or intracellular photo-catalysis? *Appl. Catal. B:*
619 *Environ.* 227, 285-295.

620 Gil Pavas, E., Correa-Sánchez, S., Acosta, D. A., 2019. Using scrap zero valent iron to replace
621 dissolved iron in the Fenton process for textile wastewater treatment: Optimization and
622 assessment of toxicity and biodegradability. *Environ. Pollut.* 252, 1709-1718.

623 Gonçalves, N. P. F., Minella, M., Fabbri, D., Calza, P., Malitesta, C., Mazzotta, E., Bianco Prevot,
624 A., 2020. Humic acid coated magnetic particles as highly efficient heterogeneous photo-
625 Fenton materials for wastewater treatments. *Chem. Eng. J.* 390, 124619.

626 Gonçalves, N. P. F., Minella, M., Mailhot, G., Brigante, M., Bianco Prevot, A., 2020. Photo-
627 activation of persulfate and hydrogen peroxide by humic acid coated magnetic particles for
628 bisphenol A degradation. *Catal. Today*, in press. DOI:
629 <https://doi.org/10.1016/j.cattod.2019.12.028>.

630 Gurkan, Y. Y., Turkten, N., Hatipoglu, A., Cinar, Z., 2012. Photocatalytic degradation of cefazolin
631 over N-doped TiO₂ under UV and sunlight irradiation: Prediction of the reaction paths via
632 conceptual DFT. *Chem. Eng. J.* 184, 113-124.

633 Hadwiger, M. E., Sommers, C. D., Mans, D. J., Patel, V., Boyne, M. T., 2012. Quality assessment
634 of U.S. marketplace vancomycin for injection products using high-resolution liquid
635 chromatography-mass spectrometry and potency assays. *Antimicrob. Agents Chemother.* 56,
636 2824–2830.

637 Hoelle, J., Johnson, J. R., Johnston, B. D., Kinkle, B., Boczek, L., Ryu, H., Hayes, S., 2019. Survey
638 of US wastewater for carbapenem-resistant Enterobacteriaceae. *J. Water Health* 17, 219-
639 226.

640 <http://www.made-in-china.com>, last accessed March 2020.

641 Huang., W., Brigante, M., Wu, F., Mousty, C., Hanna, K., Mailhot, G., 2013. Assessment of the
642 Fe(III)-EDDS complex in Fenton-like processes: from the radical formation to the
643 degradation of bisphenol A. *Environ Sci Technol.* 47, 1952-1959.

644 Hussain, G., Al-Saati, A. J., 1999. Wastewater quality and its reuse in agriculture in Saudi Arabia.
645 *Desalination* 123, 241-251.

646 Jayson, G. G., Parsons, B. J., Swallow, A. J., 1973. Some simple, highly reactive, inorganic
647 chlorine derivatives in aqueous solution. *J. Chem. Soc., Faraday I*, 1597-1607.

648 Jin, H., Tian, X., Nie, Y., Zhou, Z., Yang, C., Li, Y., Lu, L., 2017. Oxygen vacancy promoted
649 heterogeneous Fenton-like degradation of ofloxacin at pH 3.2–9.0 by Cu substituted
650 magnetic Fe₃O₄@FeOOH nanocomposite. *Environ. Sci. Technol.* 51, 12699-12706.

651 Joo, S. H., Feitz, A. J., Sedlak, D. L., Waite, T. D., 2005. Quantification of the oxidizing capacity of
652 nanoparticulate zero-valent iron. *Environ. Sci. Technol.* 39, 1263-1268.

653 Jung, Y. S., Lim, W. T., Park, J.-Y., Kim, Y.-H., 2009. Effect of pH on Fenton and Fenton-like
654 oxidation. *Environ. Technol.* 30, 183-190.

655 Keenan, C. R., Sedlak, D. L., 2008. Factors affecting the yield of oxidants from the reaction of
656 nanoparticulate zero-valent iron and oxygen. *Environ. Sci. Technol.* 42, 1262-1267.

657 Kümmerer, K., Henninger, A., 2003. Promoting resistance by the emission of antibiotics from
658 hospitals and households into effluent. *Clin. Microbiol. Infect.* 9, 1203-1214.

659 Levy, S. B., 1998. The challenge of antibiotic resistance. *Sci. Am.* 278, 46-53.

660 Li, L., Goel, R. K., 2010. Role of hydroxyl radical during electrolytic degradation of contaminants.
661 *J. Hazard. Mater.* 181, 521–525.

662 Li, L., Wei, D., Wei, G., Du, Y., 2016. Oxidation of cefazolin by potassium permanganate:
663 Transformation products and plausible pathways. *Chemosphere* 149, 279-285.

664 Liu, X., Cao, Z., Yuan, Z., Zhang, J., Guo, X., Yang, Y., He, F., Zhao, Y., Xu, J., 2018. Insight into
665 the kinetics and mechanism of removal of aqueous chlorinated nitroaromatic antibiotic
666 chloramphenicol by nanoscale zero-valent iron. *Chem. Eng. J.* 2018, 334, 508-518.

667 Lumbaque, E. C., Tiburtius, E. R. L., Barreto-Rodrigues, M., Sirtoria, C., 2019. Current trends in the
668 use of zero-valent iron (Fe^0) for degradation of pharmaceuticals present in different water
669 matrices. *Trends Environ. Anal. Chem.* 24, e00069.

670 McCullough, A. R., Parekh, S., Rathbone, J., Del Mar, C. B., Hoffmann, T. C., 2016. A systematic
671 review of the public's knowledge and beliefs about antibiotic resistance. *J. Antimicrob.*
672 *Chemother.* 71, 27-33.

673 Méndez-Arriaga, F., Esplugas, S., Giménez, J., 2010. Degradation of the emerging contaminant
674 ibuprofen in water by photo-Fenton. *Water Res.* 44, 589–595.

675 Minella, M., Bertinetti, S., Hanna, K., Minero, C., Vione, D., 2019. Degradation of ibuprofen and
676 phenol with a Fenton-like process triggered by zero-valent iron (ZVI-Fenton). *Environ Res.*
677 179, 108750.

678 Minella, M., De Bellis, N., Gallo, A., Giagnorio, M., Minero, C., Bertinetti, S., Sethi, R., Tiraferri,
679 A., Vione, D., 2018. Coupling of nanofiltration and thermal Fenton reaction for the
680 abatement of carbamazepine in wastewater. *ACS Omega* 3, 9407–9418.

681 Minella, M., Sappa, E., Hanna, K., Barsotti, F., Maurino, V., Minero, C., Vione, D., 2016.
682 Considerable Fenton and photo-Fenton reactivity of passivated zero-valent iron. RSC Adv.
683 6, 86752-86761.

684 Minero, C., Lucchiari, M., Maurino, V., Vione, D., 2013. A quantitative assessment of the
685 production of $\bullet\text{OH}$ and additional oxidants in the dark Fenton reaction: Fenton degradation
686 of aromatic amines. RSC Advances 2013, 3, 26443-26450.

687 Mirzaei, A., Chen, Z., Haghghat, F., Yerushalmi, L., 2017. Removal of pharmaceuticals from water
688 by homo/heterogeneous Fenton-type processes - A review. Chemosphere 174, 665–688.

689 National Environmental Agency, Allowable limits for trade effluent discharge to sewer/
690 watercourse/ controlled watercourse, <http://www.nea.gov.sg>, last accessed May 2016.

691 Ndieyira, J. W., Bailey, J., Patil, S. B., Vöggtli, M., Cooper, M. A., Abell, C., McKendry, R. A.,
692 Aeppli, G., 2017. Surface mediated cooperative interactions of drugs enhance mechanical
693 forces for antibiotic action. Sci. Rep. 7, 41206.

694 Neyens, E., Baeyens, J. A., 2003. A review of classic Fenton's peroxidation as an advanced
695 oxidation technique. J. Hazard. Mater. 98, 33–50.

696 Oberoi, A. S., Jia, Y. Y., Zhang, H., Khanal, S. K., Lu, H., 2019. Insights into the fate and removal
697 of antibiotics in engineered biological treatment systems: A critical review. Environ. Sci.
698 Technol. 53, 7234–7264.

699 Perini, J. A., Silva, B. F., Nogueira, R. F., 2014. Zero-valent iron mediated degradation of
700 ciprofloxacin - assessment of adsorption, operational parameters and degradation products.
701 Chemosphere 117, 345-352.

702 Perl, T. M., 1999. The threat of vancomycin resistance. Am. J. Med. 106, 26S-37S.

703 Piddock, L. J. V., 2011. The crisis of no new antibiotics - what is the way forward? Lancet Infect.
704 Dis. 12, 249-253.

705 Pignatello, J. J., Liu, D., Huston, P., 1999. Evidence for an additional oxidant in the photoassisted
706 Fenton reaction. Environ. Sci. Technol. 33, 1832–1839.

707 Pignatello, J. J., Oliveros, E., MacKay, A., 2006. Advanced oxidation processes for organic
708 contaminant destruction based on the Fenton reaction and related chemistry. *Crit. Rev.*
709 *Environ. Sci. Technol.* 36, 1–84.

710 Polesel, F., Andersen, H. R., Trapp, S., Plósz, B. G., 2016. Removal of antibiotics in biological
711 wastewater treatment systems - A critical assessment using the activated sludge modeling
712 framework for xenobiotics (ASM-X). *Environ. Sci. Technol.* 50, 10316-10334.

713 Qian, M., Yang, L., Chen, X., Li, K., Xue, W., Li, Y., Zhao, H., Cao, G., Guan, X., Shen, G., 2020.
714 The treatment of veterinary antibiotics in swine wastewater by biodegradation and Fenton-
715 like oxidation. *Sci. Total Environ.* 710, 136299.

716 Rattie, E. S., Ravin, L. J., 1975. Pharmacokinetic interpretation of blood levels and urinary
717 excretion data for cefazolin and cephalothin after intravenous and intramuscular
718 administration in humans. *Antimicrob. Agents Chemother.* 7, 606-613.

719 Rezaei, F., Vione, D., 2018. Effect of pH on zero valent iron performance in heterogeneous Fenton
720 and Fenton-like processes: A review. *Molecules* 23, E3127.

721 Ricceri, F., Giagnorio, M., Farinelli, G., Blandini, G., Minella, M., Vione, D., Tiraferri, A., 2019.
722 Desalination of produced water by membrane distillation: Effect of the feed components and
723 of a pre-treatment by Fenton oxidation. *Sci Rep.* 9, 14964.

724 Richardson, S. D., Ternes, T. A., 2018. Water analysis: emerging contaminants and current issues.
725 *Anal. Chem.* 90, 398-428.

726 Rizzo, L., Gernjak, W., Krzeminski, P., Malato, S., McArdell, C. S., Perez, J. A. S., Schaar, H.,
727 Fatta-Kassinos, D., 2020. Best available technologies and treatment trains to address current
728 challenges in urban wastewater reuse for irrigation of crops in EU countries. *Sci. Total*
729 *Environ.* 710, 136312.

730 Rizzo, L., Manaia, C., Merlin, C., Schwartz, T., Dagot, C., Ploy, M. C., Michael, I., Fatta-Kassinos,
731 D., 2013. Urban wastewater treatment plants as hotspots for antibiotic resistant bacteria and
732 genes spread into the environment: A review. *Sci Total Environ.* 447, 345-60.

733 Roche, M., Bornet, C., Monges, P., Stein, A., Gensollen, S., Seng, P., 2016. Misuse of antibiotics
734 reserved for hospital settings in outpatients: a prospective clinical audit in a university
735 hospital in Southern France. *Int. J. Antimicrob. Agents* 48, 96-100.

736 Salgota, M., Huertasa, E., Weber, S., Dott, W., Hollender, J., 2006. Wastewater reuse and risk:
737 definition of key objectives. *Desalination* 187, 29-40.

738 Sandell, E. B., 1950. *Colorimetric Determination of Traces of Metals*. Vol. 3, 2nd ed. New York:
739 Interscience Publishers, 688 pp.

740 Shams El Din, A. M., Mohammed, R. A., 1998. Kinetics of the reaction between hydrogen peroxide
741 and hypochlorite. *Desalination* 115, 145-153.

742 Sharma, V. K., Johnson, N., Cizmas, L., McDonald, T. J., Kim, H., 2016. A review of the influence
743 of treatment strategies on antibiotic resistant bacteria and antibiotic resistance genes.
744 *Chemosphere* 150, 702-714.

745 Takata, N., Suginaka, H., Kotani, S., Ogawa, M., Kosaki, G., 1981. β -Lactam resistance in *Serratia*
746 *marcescens*: comparison of action of benzylpenicillin, apalcillin, cefazolin, and ceftizoxime.
747 *Antimicrob. Agents Chemother.* 19, 397-401.

748 Tang, J. T., Wang, J. L., 2020. Iron-copper bimetallic metal-organic frameworks for efficient
749 Fenton-like degradation of sulfamethoxazole under mild conditions. *Chemosphere* 241,
750 125002.

751 von Gunten, U., 2018. Oxidation processes in water treatment: Are we on track? *Environ. Sci.*
752 *Technol.* 52, 5062-5075.

753 Vorontsov, A. V., 2019. Advancing Fenton and photo-Fenton water treatment through the catalyst
754 design. *J. Hazard. Mater.* 372, 103-112.

755 Wang, J., Zhuan, R., 2020. Degradation of antibiotics by advanced oxidation processes: An
756 overview. *Sci. Total Environ.* 701, 135023.

757 Wiles, S., 2015. All models are wrong, but some are useful: Averting the 'microbial apocalypse'.
758 *Virulence* 6, 730-732.

759 Wright, H., Bonomo, R. A., Paterson, D. L., 2017. New agents for the treatment of infections with
760 Gram-negative bacteria: restoring the miracle or false dawn? *Clin. Microbiol. Infect.* 23,
761 704-712.

762 Wu, Y., Bianco, A., Brigante, M., Dong, W., de Sainte-Claire, P., Hanna, K., Mailhot, G., 2015.
763 Sulfate radical photogeneration using Fe-EDDS: Influence of critical parameters and
764 naturally occurring scavengers. *Environ. Sci. Technol.* 49, 14343-14349.

765 Xu, J., Cao, Z., Wang, Y., Zhang, Y., Gao, X., Ahmed, M. B., Zhang, J., Yang, Y., Zhou, J. L.,
766 Lowry, G. V., 2019. Distributing sulfidized nanoscale zerovalent iron onto
767 phosphorusfunctionalized biochar for enhanced removal of antibiotic florfenicol. *Chem.*
768 *Eng. J.* 359, 713-722.

769 Xu, J., Liu, X., Cao, Z., Bai, W., Shi, Q., Yang, Y., 2020. Fast degradation, large capacity, and high
770 electron efficiency of chloramphenicol removal by different carbon-supported nanoscale
771 zerovalent iron. *J. Hazard. Mater.* 384, 121253.

772 Zhang, M. H., Dong, H., Zhao, L., Wang, D. X., Meng, D., 2019. A review on Fenton process for
773 organic wastewater treatment based on optimization perspective. *Sci Total Environ.* 670,
774 110-121.

775 Zhao, H., Cao, Z., Liu, X., Zhan, Y., Zhang, J., Xiao, X., Yang, Y., Zhou, J., Xu, J., 2017. Seasonal
776 variation, flux estimation, and source analysis of dissolved emerging organic contaminants
777 in the Yangtze Estuary, China. *Mar. Pollut. Bull.* 125, 208-215.

778 Zhong, Y., Liang, X., Zhong, Y., Zhu, J., Zhu, S., Yuan, P., He, H., Zhang, J., 2012. Heterogeneous
779 UV/Fenton degradation of TBBPA catalyzed by titanomagnetite: Catalyst characterization,
780 performance and degradation products. *Water Res.* 46, 4633-4644.

Table 1. Assessment of treatment costs for chemical reagents, required to treat WWa and WWb with ZVI-Fenton at initial pH 5. Note that conventional treatment would cost around 0.4 \$ m⁻³, to which these are added costs.

	Cost, \$ m⁻³	
	WWa	WWb
ZVI	0.016	0.016
H₂O₂	0.012	0.012
H₂SO₄	0.008	0.038
Total cost	0.036	0.066

Captions to figures and schemes

Figure 1. Degradation of a mixture of $4 \mu\text{mol L}^{-1}$ CFZ + $4 \mu\text{mol L}^{-1}$ VNM + $4 \mu\text{mol L}^{-1}$ IMI in ultra-pure water, in the presence of ZVI + H_2O_2 (solid symbols) and of ZVI alone (open symbols). (a) pH 5 by PB, $100 \mu\text{mol L}^{-1}$ H_2O_2 per addition, 0.01 g L^{-1} ZVI; (b) pH 6 by PB, $200 \mu\text{mol L}^{-1}$ H_2O_2 per addition, 0.03 g L^{-1} ZVI; (c) pH 7 by PB, $200 \mu\text{mol L}^{-1}$ H_2O_2 per addition, 0.04 g L^{-1} ZVI. PB: phosphate buffer ($\text{H}_3\text{PO}_4 + \text{NaH}_2\text{PO}_4$) 0.001 mol L^{-1} . The vertical arrows highlight the time of the second addition of H_2O_2 , in the case of the ZVI + H_2O_2 runs.

The pseudo-first order rate constants k of antibiotic degradation, obtained by fitting the curves with a mono-exponential equation, are as follows (error bounds represent $\pm\sigma$, value in brackets refer to runs with ZVI alone).

pH	k, min^{-1}		
	CFZ	IMI	VNM
5	0.49 ± 0.05 (0.004 ± 0.001)	0.41 ± 0.05 (0.002 ± 0.001)	0.45 ± 0.08 (0.005 ± 0.001)
6	0.26 ± 0.05 (0.005 ± 0.001)	0.15 ± 0.03 (0.0015 ± 0.0006)	0.32 ± 0.09 (0.008 ± 0.001)
7	0.09 ± 0.01 (0.018 ± 0.001)	0.07 ± 0.01 (0.002 ± 0.001)	0.16 ± 0.02 (0.019 ± 0.001)

Figure 2. Degradation of a mixture of $4 \mu\text{mol L}^{-1}$ CFZ + $4 \mu\text{mol L}^{-1}$ VNM + $4 \mu\text{mol L}^{-1}$ IMI at pH 5, adjusted by H_2SO_4 before the beginning of the reaction and corrected again at 30 min. (a) WWa. (b) WWb. Conditions used in both cases: 0.02 g L^{-1} ZVI; $400 \mu\text{mol L}^{-1}$ H_2O_2 added in three aliquots ($300 \mu\text{mol L}^{-1}$ at 0 min, $50 \mu\text{mol L}^{-1}$ at 30 min, and $50 \mu\text{mol L}^{-1}$ at 60 min). The solid vertical arrows highlight the times of further additions of H_2O_2 . The dotted vertical arrow highlights the time of pH correction (H_2SO_4). Solid symbols: ZVI + H_2O_2 ; open symbols: ZVI alone. WWa had $270 \mu\text{S cm}^{-1}$ conductivity, pH 7.5 and $7.8 \text{ mg}_\text{C} \text{ L}^{-1}$ TOC. The corresponding parameters for WWb were $900 \mu\text{S cm}^{-1}$, 7.8 and $38.9 \text{ mg}_\text{C} \text{ L}^{-1}$.

WW type	k, min^{-1}		
	CFZ	IMI	VNM
WWa	0.049±0.006 (0.003±0.001)	0.048±0.007 (negligible)	0.030±0.005 (0.003±0.001)
WWb	0.081±0.012 (0.002±0.001)	0.106±0.015 (negligible)	0.036±0.005 (0.002±0.001)

Scheme 1. Tentative reaction schemes to account for the ZVI-Fenton transformation of the studied antibiotics (**a**: CFZ; **b**: IMI; **c**: VNM) into the detected reaction intermediates (P#). The dashed arrows indicate very tentative pathway proposals.

Figure 1

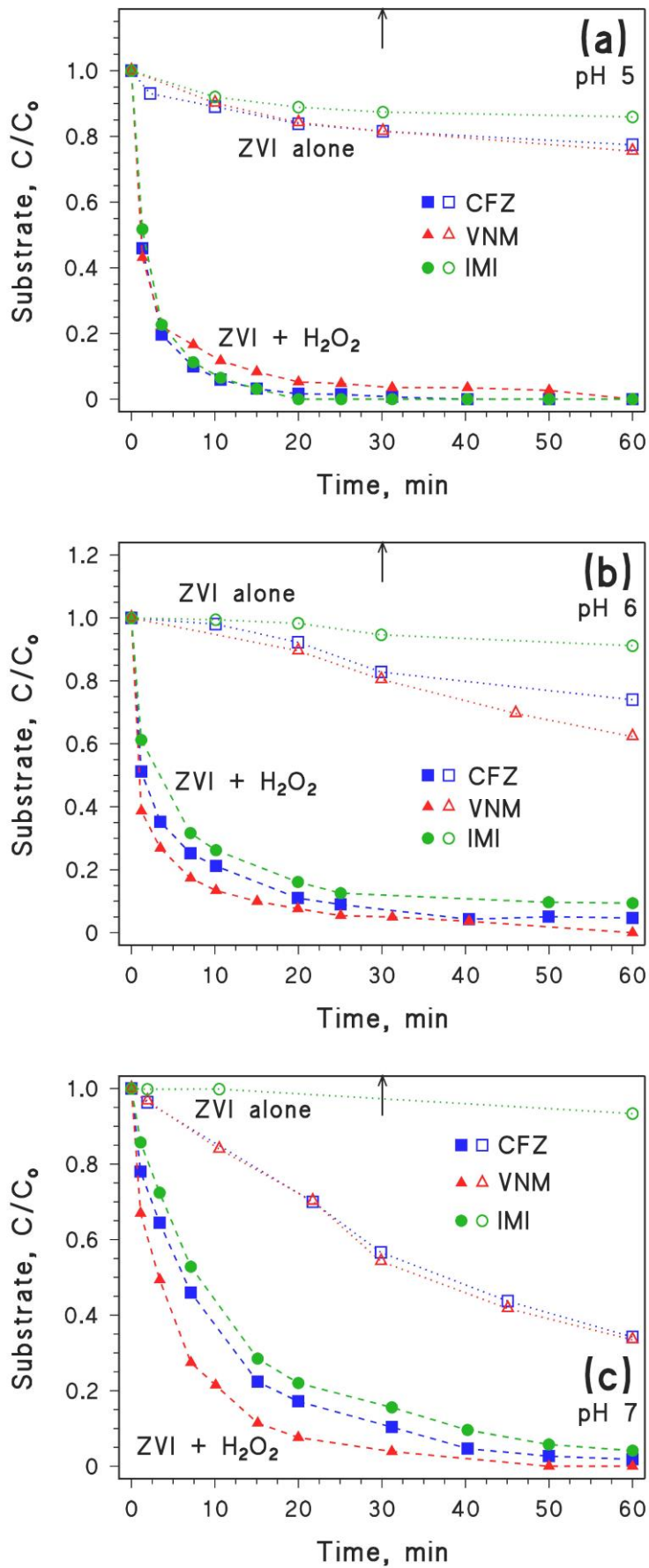
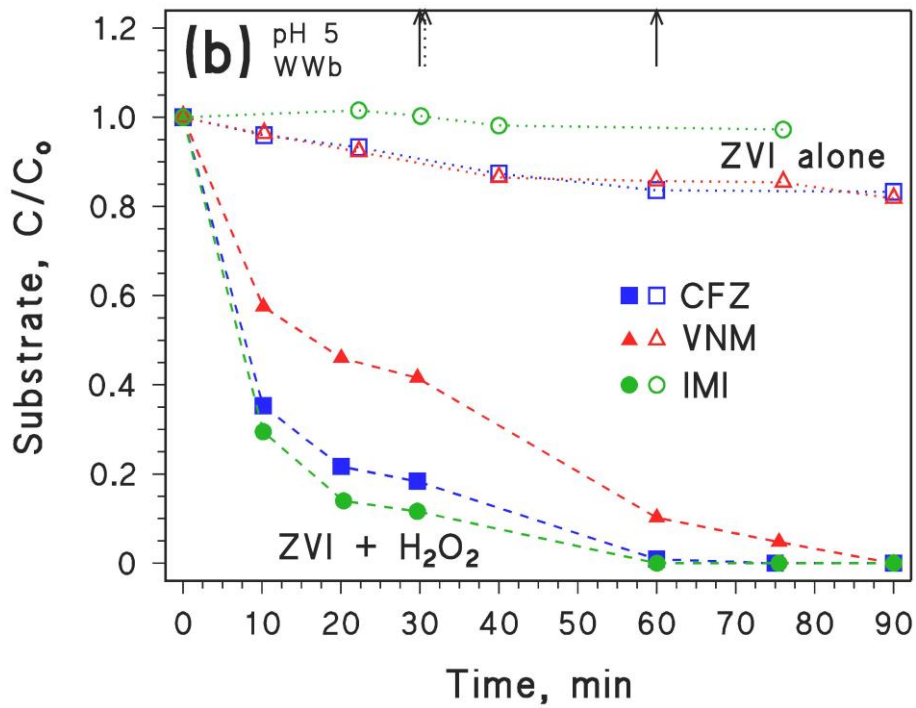
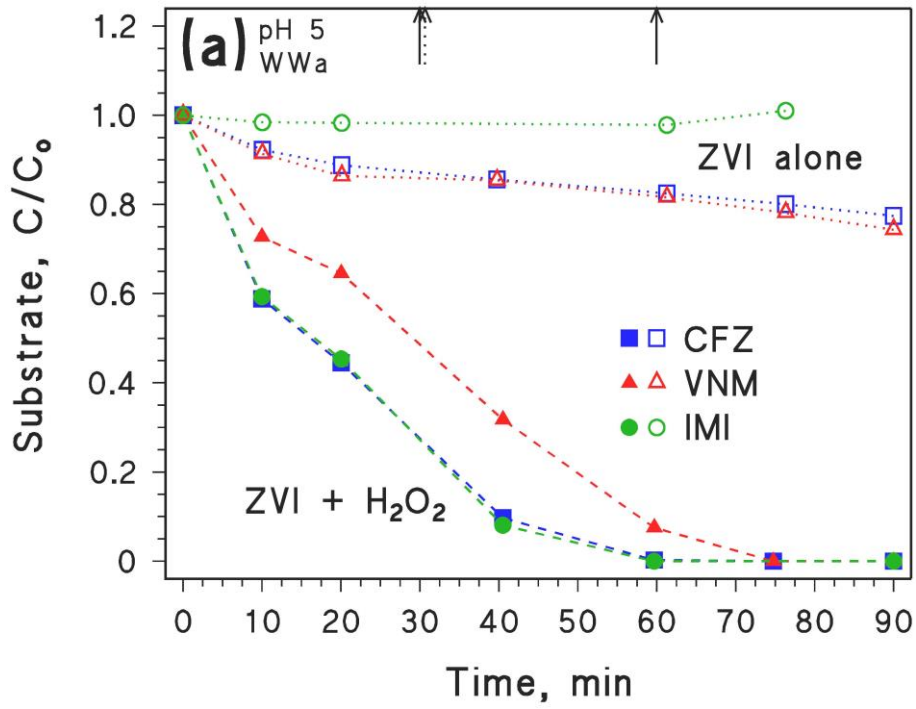


Figure 2



Scheme 1

